# Hunt for a Lifshitz point in single-crystalline $UPd_2Si_2$. II. High pressures

Maria Szlawska,[1,*] Magdalena Majewicz,[1] Masashi Ohashi,[1,2] and Dariusz Kaczorowski[1]
[1]*Institute of Low Temperature and Structure Research, Polish Academy of Sciences, ul. Okólna 2, 50-422 Wrocław, Poland*
[2]*Institute of Science and Engineering, Kanazawa University, Kakuma-machi, Kanazawa 920-1192, Japan*

(Received 13 May 2024; accepted 8 July 2024; published 23 July 2024)

A single crystal of $UPd_2Si_2$ was studied in wide ranges of temperature, magnetic field strength, and hydrostatic pressure with the main aim of revealing the existence of a Lifshitz point in its magnetic phase diagram. The experiments showed that up to 14 T and 7 GPa, the boundaries between paramagnetic, modulated, and uniform magnetic phases do not meet. The application of external pressure leads to stabilization of the antiferromagnetic phase. Simultaneously, the triple point in the $H$-$T$ phase diagram, where the ferrimagnetic phase emerges, is shifted to higher fields. This finding is discussed with respect to two different magnetic phase diagrams of $UPd_2Si_2$ reported in the literature.

DOI: 10.1103/PhysRevB.110.014435

## I. INTRODUCTION

A Lifshitz point (LP) is a special multicritical point, whose concept was introduced by Hornreich, Luban, and Shtrickman [1,2]. In the case of a magnetic system, a disordered paramagnetic phase meets at LP with two ordered phases—incommensurately modulated and uniform. In other words, LP is a point, which divides a continuous transition line into two segments: one separating the paramagnetic phase from the incommensurate phase, and another one being a borderline between the paramagnetic state and the uniform phase. To date, the presence of LP was conclusively shown only for MnP [3].

The U-based silicides with composition $UT_2Si_2$ (where $T$ is a $d$-electron transition element) can adopt two closely related tetragonal crystal structures: $ThCr_2Si_2$ type or $CaBe_2Ge_2$ type. Both types are notably elongated along the tetragonal $c$ axis [4]. These compounds exhibit a large variety of physical behaviors, including Pauli paramagnetism [5,6], various types of magnetic ordering [7–19], or the famous "hidden-order" state [20]. The magnetic moments, originated from the $5f$ electronic shell of U atoms (the only exception is the Mn-bearing phase [9]), align along the $c$ axis. Some of these compounds exhibit magnetic phase diagrams that are rich with phases [11,21,22]. Inelastic x-ray scattering revealed that the ground state of the $UT_2Si_2$ silicides is predominantly driven by the varying degrees of localization of $5f$ electrons [23].

The U-based silicide $UPd_2Si_2$ has previously attracted a lot of attention due to its complex magnetic behavior. The compound crystallizes with a tetragonal crystal structure of the $ThCr_2Si_2$ type (s.g. $I4/mmm$), in which U, Pd, and Si atoms form layers, stacking along the fourfold tetragonal axis. The magnetic moments carried by U atoms are oriented along the $c$ axis of the unit cell [24,25]. The $H$-$T$ magnetic phase diagram determined for the magnetic field $H \parallel c$ consists of four domains: paramagnetic (PM), incommensurately modulated sine wave (IC), simple antiferromagnetic (AFM), and ferrimagnetic (FIM) [26]. Noticeably, two different magnetic phase diagrams of the compound can be found in the literature [21,22], which basically differ in the number of magnetic phase transitions observed in zero field. In both cases, the application of a magnetic field stabilizes the FIM ordering. Furthermore, the IC area domain gets narrower with increasing magnetic field strength, and it is expected that in high enough fields, the boundary lines between PM, IC, and FIM phases meet at a single point, which can be a Lifshitz point [22]. Interestingly, it was reported that hydrostatic pressure stabilizes the AFM ordering in $UPd_2Si_2$ [27–29]. The experiments performed up to 4.2 GPa in zero magnetic field revealed that the temperature of the transition between the IC and AFM phases increases with increasing pressure, while the Néel temperature does not change. In consequence, near 3.4 GPa, the boundary lines between the AFM, IC, and PM phases meet at a putative pressure-induced LP [29].

With the main aim to verify the hypothesis of the existence of LP in the magnetic phase diagrams of $UPd_2Si_2$, we have undertaken own studies of the compound. In our companion paper [30], we presented the results of our examination of the physical properties of $UPd_2Si_2$, focused at the high-field region. We have obtained a magnetic phase diagram, similar to that presented by Honma *et al.* [21]. In zero field, we observed two magnetic phase transitions, namely from PM to IC at 132 K, and from IC to AFM at 108 K. The application of the magnetic field resulted in the formation of FIM. The triple point (TP), at which the three ordered phases meet, was found near the field 2 T at the temperature 106 K. The magnetic field leads to narrowing the area of the FIM phase. However, the boundary lines between the FIM, IC, and PM phases do not meet up to 14 T, mainly because the Néel temperature increases slightly in the highest magnetic fields examined. In this paper, we address the magnetotransport behavior in

*Contact author: m.szlawska@intibs.pl

 

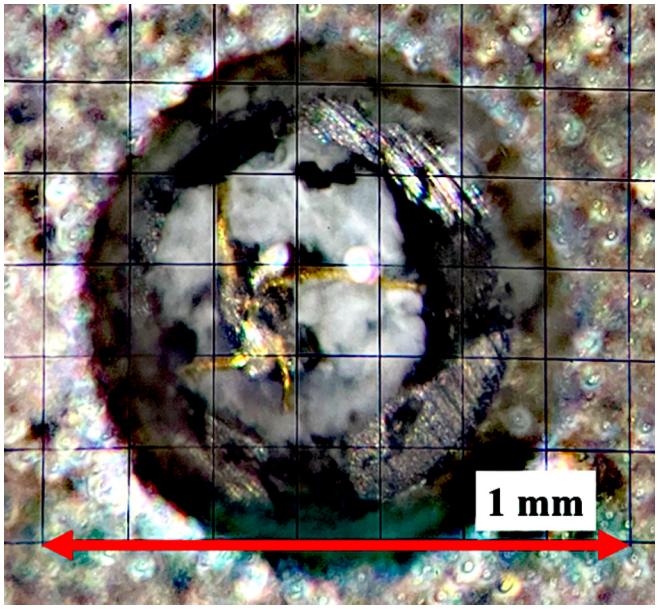


FIG. 1. $UPd_2Si_2$ sample prepared for electrical resistivity measurements in the pressure cell.

$UPd_2Si_2$ studied in high magnetic fields under high-pressure conditions.

## II. EXPERIMENTAL DETAILS

A single crystal of $UPd_2Si_2$ was grown using the Czochralski pulling technique in a tetra-arc furnace (GES Corporation) under argon atmosphere. The details of the growing process and crystal-chemical characterization of the obtained material are given in the companion paper [30].

The temperature and magnetic field variations of the electrical resistivity at high pressures were measured with the electric current flowing perpendicular to the $c$ axis and magnetic field applied along it. For these experiments a specimen was loaded into a sample chamber made from a stainless steel gasket (see Fig. 1). Four gold wires (diameter 17.5 μm) were connected to the sample by spot welding. The gasket was squeezed between the flats of two opposed anvils made of tungsten carbide and the sample and liquid pressure medium (1:1 mixture of Fluorinert FC43, and FC72) were enclosed. Shallow grooves were milled into the lower anvil in order to introduce electrical leads into the sample chamber. The grooves were filled with alumina powder and STYCAST 2850FT which ensured electrical insulation, as well as sealing off the sample chamber. The load on the anvils, and hence the pressure in the cell, was changed at room temperature and kept constant when the temperature was lowered. The pressure in the sample chamber was determined as a function of load by measuring beforehand the superconducting

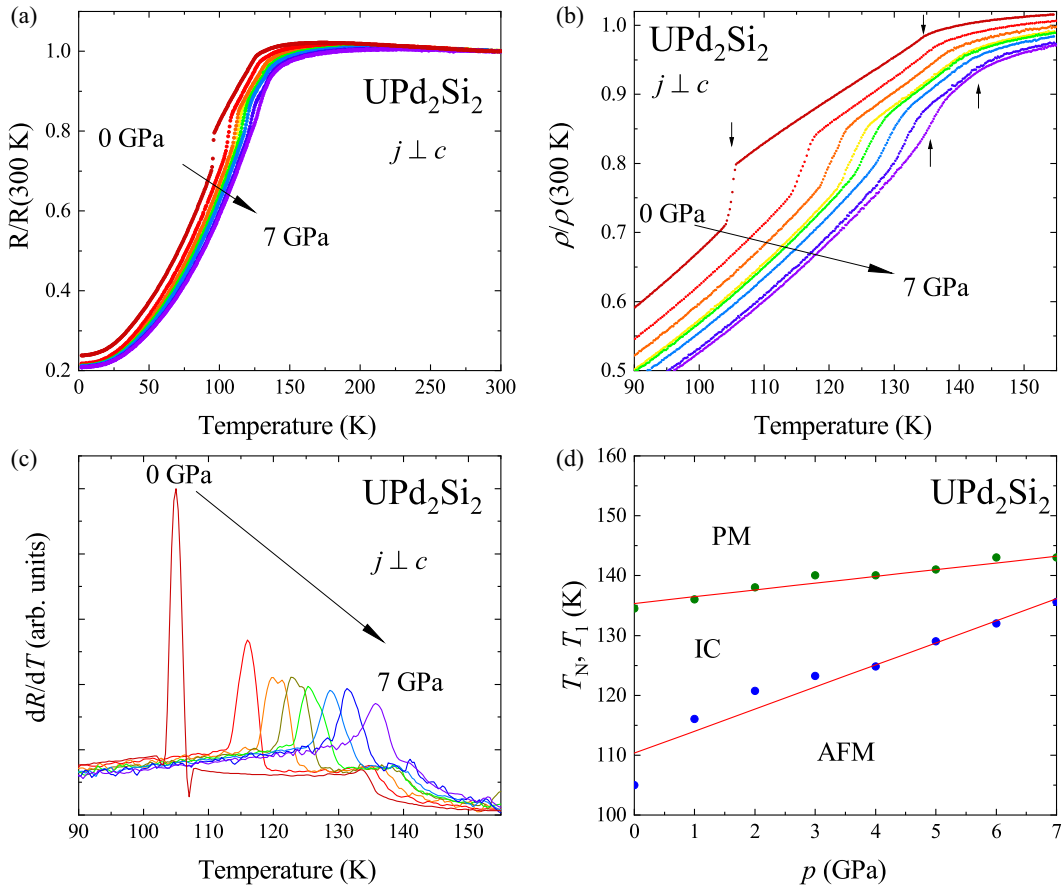


FIG. 2. (a), (b) Temperature dependence of the electrical resistivity of single-crystalline $UPd_2Si_2$, measured with $j \perp c$ in high pressures from 1 to 7 GPa varying in 1 GPa increments (a) in the wide temperature range and (b) in the vicinity of the magnetic phase transitions. The arrows in (b) mark the magnetic phase transitions for the variations taken at 1 and 7 GPa. (c) The temperature derivative of the electrical resistivity variations. (d) The pressure-temperature magnetic phase diagram of $UPd_2Si_2$.

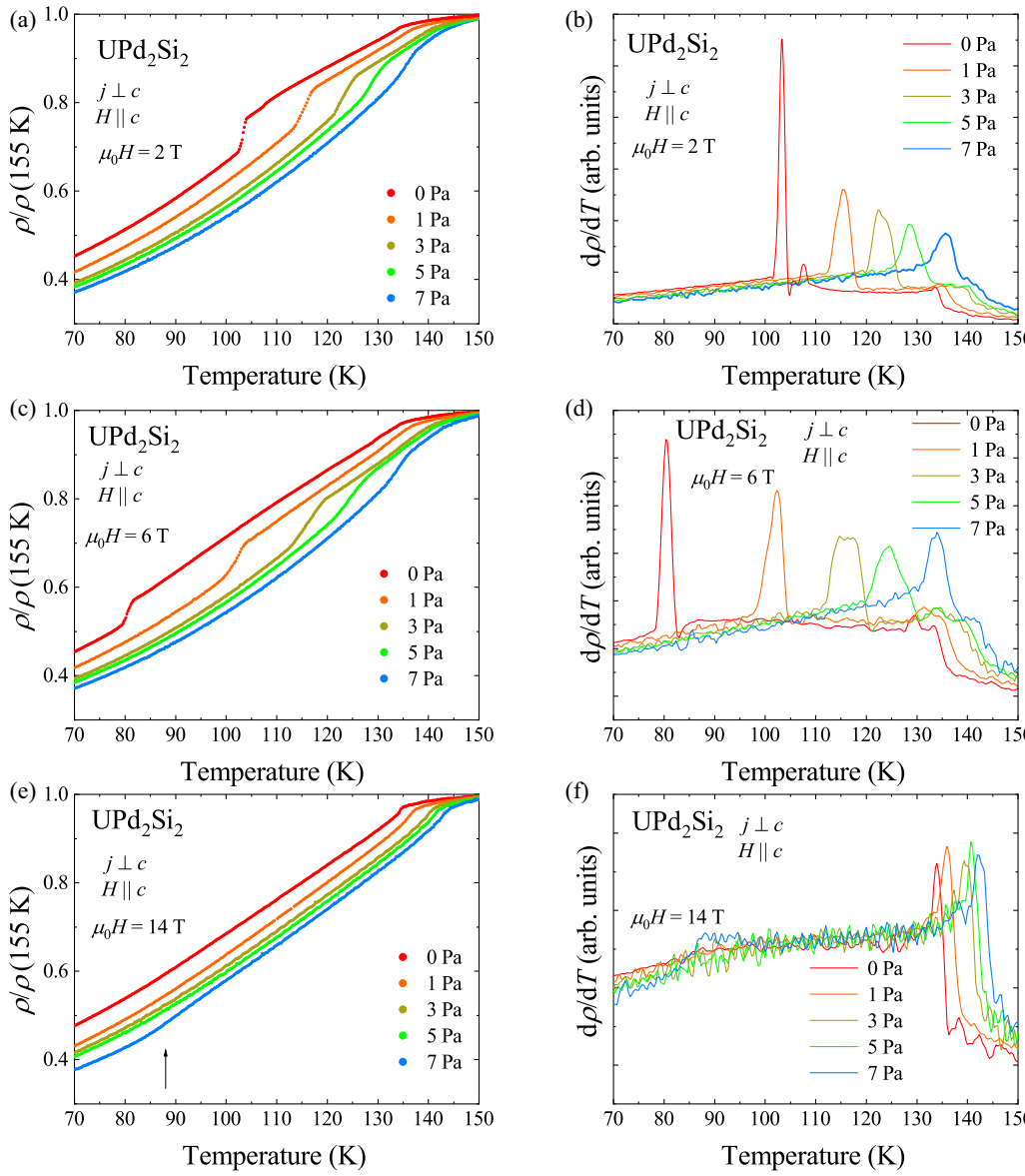


FIG. 3. (a), (c), and (e) Temperature dependencies of the electrical resistivity of $UPd_2Si_2$ measured with $j \perp c$ and with magnetic fields of 2, 6, and 14 T, respectively, applied along the $c$ axis, in high pressures. The arrow in (e) marks the first-order phase transition between FIM and AFM phases. (b), (d), and (f) Temperature derivatives of the electrical resitivity.

transition temperature of lead in the same pressure cell [31]. For these experiments a Quantum Design Physical Property Measurement System (PPMS-14) platform was used.

## III. RESULTS AND DISCUSSION

### A. Experiments in zero magnetic field

In order to observe the pressure-induced LP in $UPd_2Si_2$, described before in the literature [27–29], the electrical resistivity was measured for the single-crystalline specimen mounted in the high-pressure cell. Figure 2(a) presents the temperature dependencies of the resistivity normalized to 300 K, taken for pressures up to 7 GPa in the temperature range from 2 to 300 K. The resistivity in the vicinity of magnetic phase transitions is presented in Fig. 2(b). In contrast to the previous report [29], the overall character of the $\rho(T)$ variations does not change. In all the curves, the magnetic phase transition at $T_N$ manifests itself as a kink, that corresponds to an inflection point in the temperature derivative of the resistivity $d\rho/dT$ and a minimum in the second-order derivative $d^2\rho/dT^2$. The first-order transition to the antiferromagnetic state at $T_{\text{IC-AFM}}$ is seen as a drop in $\rho(T)$. With increasing pressure, the value of $T_{\text{IC-AFM}}$, determined as a maximum in the first temperature derivative of the resistivity $d\rho/dT$ [see Fig. 2(c)], increases monotonically, in agreement with the previous reports [27–29], and the step associated with the phase transition gradually broadens. On the other hand, the kink at the Néel temperature is less pronounced and somewhat shifts towards higher temperatures with increasing pressure, reaching a value of 143 K at 7 GPa. As a result, at odds with Refs. [28,29], the phase transition lines between the PM-IC and IC-AFM phases do not meet up to the highest

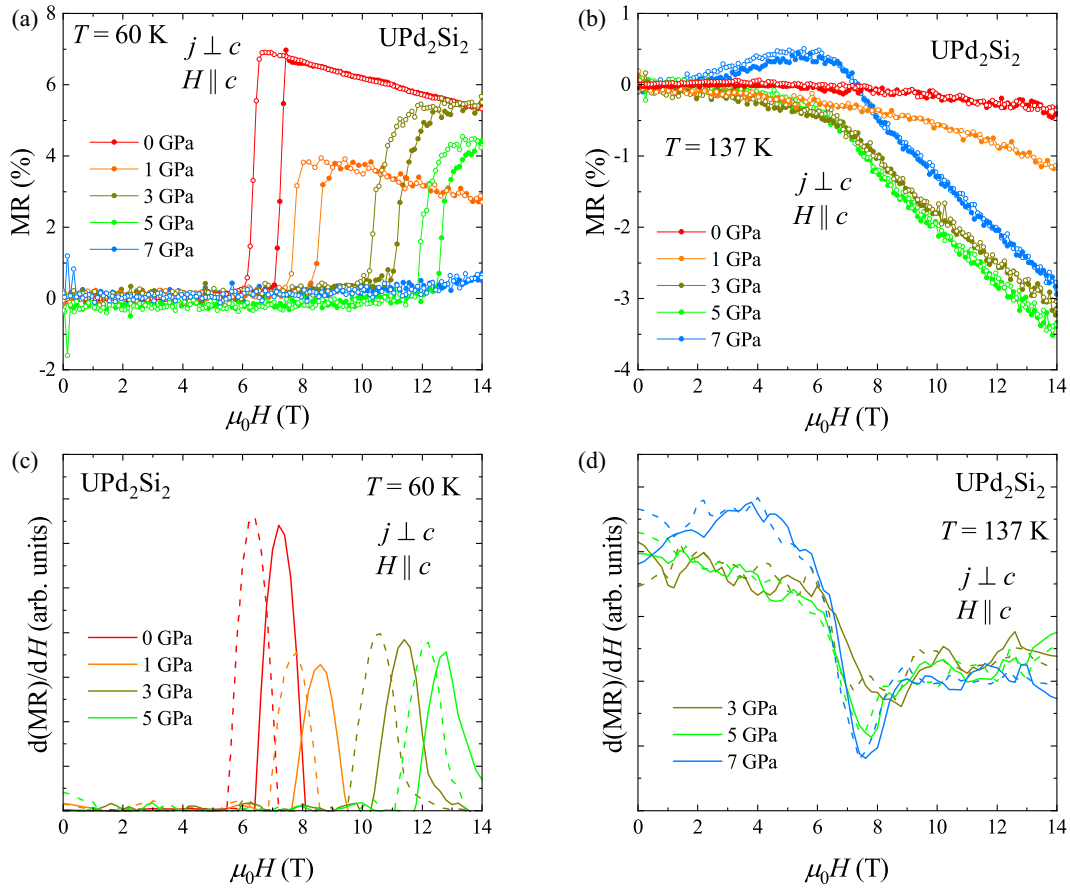


FIG. 4. (a) and (b) Magnetoresistivity of $UPd_2Si_2$ as a function of the magnetic field strength applied along the $c$ axis, measured with $j \perp c$ at a constant temperature of 60 and 137 K, respectively, in high pressures. Solid and open symbols denote variations measured with increasing and decreasing magnetic field, respectively. (c) and (d) Field derivatives of the magnetoresistivity. Solid and dashed lines denote the curves determined for increasing and decreasing magnetic field, respectively.

pressures applied. However, as the change in the position of $T_N$ is small, such a merger of the two phase boundaries may occur beyond that limit. The resistivity data collected in the present study were used to construct the pressure-temperature phase diagram of $UPd_2Si_2$, which is shown in Fig. 2(d).

### B. Experiments in finite magnetic fields

#### *1. Temperature variations of the resistivity*

Figure 3 illustrates the effect of external pressure on the resistivity of $UPd_2Si_2$ measured within the basal tetragonal plane, in magnetic fields applied along the $c$ axis. As seen in Fig. 3(a), at ambient pressure, the $\rho(T)$ variation measured in $\mu_0 H = 2$ T exhibits three phase transitions. With decreasing temperature, $\rho(T)$ first bends downwards at $T_N$, then it shows a tiny step associated with a transition from the IC to the FIM phase at $T_{\text{IC-FIM}} = 108$ K, and a large step that manifests the onset of the AFM ordering at $T_{\text{FIM-AFM}} = 103$ K. The two latter transitions can be recognized as maxima in the temperature derivative of the resistivity [see Fig. 3(b)]. The increase of pressure leads to the disappearance of the phase transition to the FIM phase, which is no longer observed for $p \geqslant 1$ GPa. Furthermore, in higher pressures, $T_{\text{IC-AFM}}$ increases significantly, while $T_N$ increases only slightly.

The $\rho(T)$ dependencies measured in $\mu_0 H = 6$ T and their temperature derivatives are shown in Figs. 3(c) and 3(d), respectively. At ambient pressure three magnetic phase transitions at $T_N$, $T_{\text{IC-FIM}}$, and $T_{\text{FIM-AFM}}$ can be recognized. With increasing pressure a kink associated with $T_N$ moves slightly towards higher temperatures. In turn, the drop associated with the transition to the simple AFM state broadens and shifts towards higher temperatures. The small maximum in $d\rho/dT$, just below $T_N$, associated with the IC-FIM transition, initially shifts slightly towards higher temperatures and finally is not observed for $p = 7$ GPa. At this pressure only two phase transitions at $T_N = 142$ K and $T_{\text{IC-AFM}} = 134$ K are observed, and the FIM phase is not formed.

In $\mu_0 H = 14$ T [see Figs. 3(e) and 3(f)], the overall character of all the $\rho(T)$ curves hardly changes with changing pressure. The kink marking $T_N$ shifts towards higher temperatures with increasing pressure and simultaneously, a maximum in $d\rho/dT(T)$ associated with the transition between the IC and FIM phases shifts towards higher temperatures. The transition lines between the IC-FIM and FIM-AFM phases do not merge up to 7 GPa. It is worthwhile noting that the $\rho(T)$ variation measured in the latter pressure shows a broad and small drop at about 90 K. This feature is well seen as a broad maximum in the temperature derivative of the

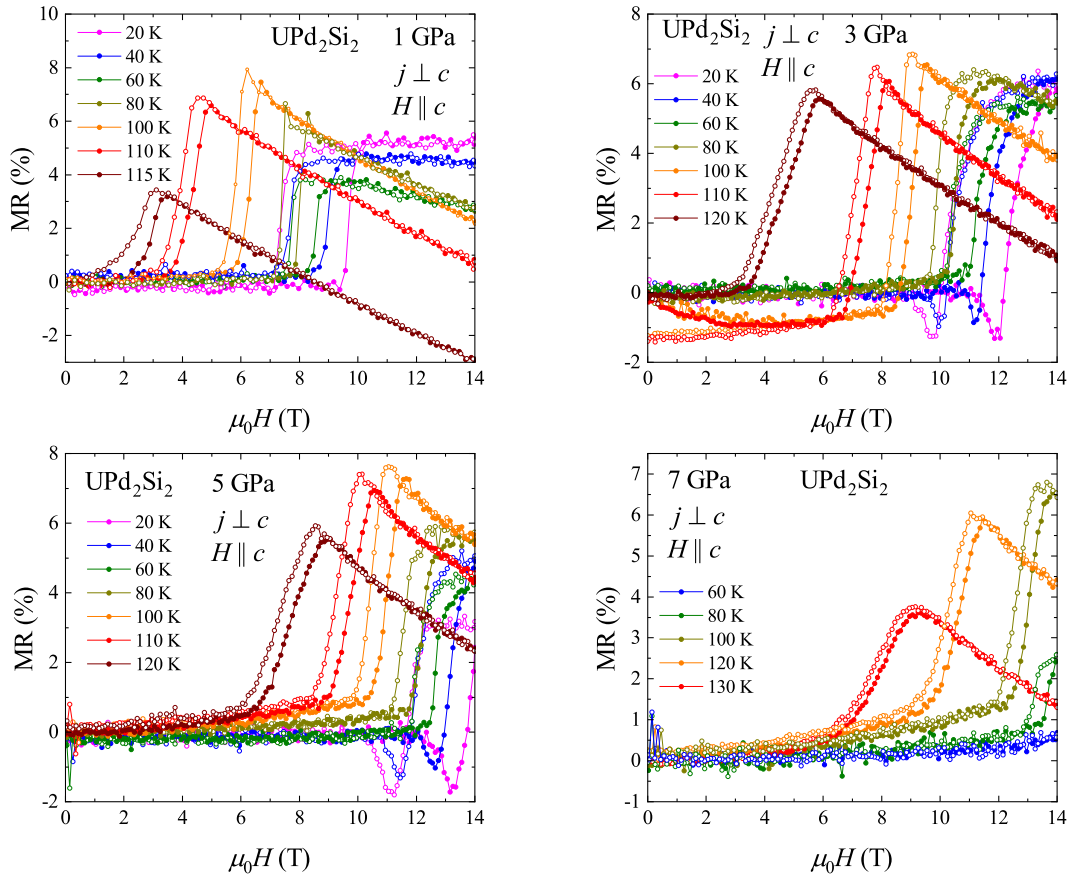


FIG. 5. Field dependencies of the magnetoresistivity of single-crystal $UPd_2Si_2$, measured with $j \perp c$ and $B \parallel c$ at different temperatures below $T_{\text{IC-AFM}}$, in high pressures. Solid and open symbols denote variations measured with increasing and decreasing magnetic field, respectively.

resistivity and signals the onset of the AFM state, that at 7 GPa can be observed in magnetic fields as high as 14 T. Noticeably, external pressure stabilizes the AFM phase in $UPd_2Si_2$ and shifts TP between the AFM, IC, and FIM phases in the $H$-$T$ phase diagram towards higher magnetic fields.

### 2. *Field variations of the magnetoresistivity*

The influence of high pressure on the $H$-$T$ phase diagram of $UPd_2Si_2$ can be also determined from the magnetic field variations of the magnetoresistivity, defined as $\text{MR}(H) = \frac{\rho(H)-\rho(0)}{\rho(0)}$. Figure 4 presents the magnetoresistivity isotherms recorded at selected temperatures under different pressures. Figure 4(a) shows the MR vs $H$ data measured at 60 K, that is much below $T_{\text{IC-AFM}}$. As can be inferred from the figure, the metamagnetic transition from the AFM to FIM phase manifests itself as a rapid increase in MR. The critical field, defined as an inflection point in the $\text{MR}(H)$ variations [maxima in the field derivatives of MR, displayed in Fig. 4(c)], systematically increases with increasing pressure. Finally, at a terminal pressure of 7 GPa, no metamagnetic feature is observed and the compound remains antiferromagnetic up to 14 T. This behavior confirms the stabilization of the antiferromagnetic phase in $UPd_2Si_2$ by applying pressure.

Figure 4(b) shows the MR isotherms recorded at 137 K, i.e., above $T_{\text{IC-AFM}}$. At ambient pressure, $\text{MR}(H)$ is featureless and characteristic of paramagnets. As discussed in Sec. III A, with rising pressure, the ordering temperature $T_N$ increases, yet with a smaller rate than $T_{\text{IC-AFM}}$. The $\text{MR}(H)$ dependencies measured under pressures of 3 and 5 GPa, exhibit a slight drop associated with a transition between the IC and FIM phases [$H_c$ was defined as a minimum in the field derivatives of MR; see Fig. 4(d)]. At 7 GPa, $\text{MR}(H)$ shows slightly different behavior, probably because of the closeness of the transition at $T_{\text{IC-AFM}}$. With increasing magnetic field, MR initially increases, goes through a wide maximum, and then decreases, showing finally the metamagnetic transition from the IC to FIM phases. The metamagnetic transitions in both temperature regions show clear hysteresis, characteristic of first-order type transitions.

The field dependencies of the magnetoresistivity measured at different temperatures below $T_{\text{IC-AFM}}$ at pressures 1, 3, 5, and 7 GPa are shown in Fig. 5. Overall, the $\text{MR}(H)$ curves measured up to 5 GPa are similar. At 20 K, they show a wide hysteresis, associated with the metamagnetic transition. With increasing temperature, the loops become narrower and shift towards smaller magnetic fields. With increasing pressure, the isotherms move towards higher magnetic fields, due to the stabilization of the AFM phase. One observes a shift towards higher fields of the triple point, in which the three ordered phases meet. At 20 K, the critical field increases from 10 T for 1 GPa to 12 T for 5 GPa (at ambient pressure, it was equal

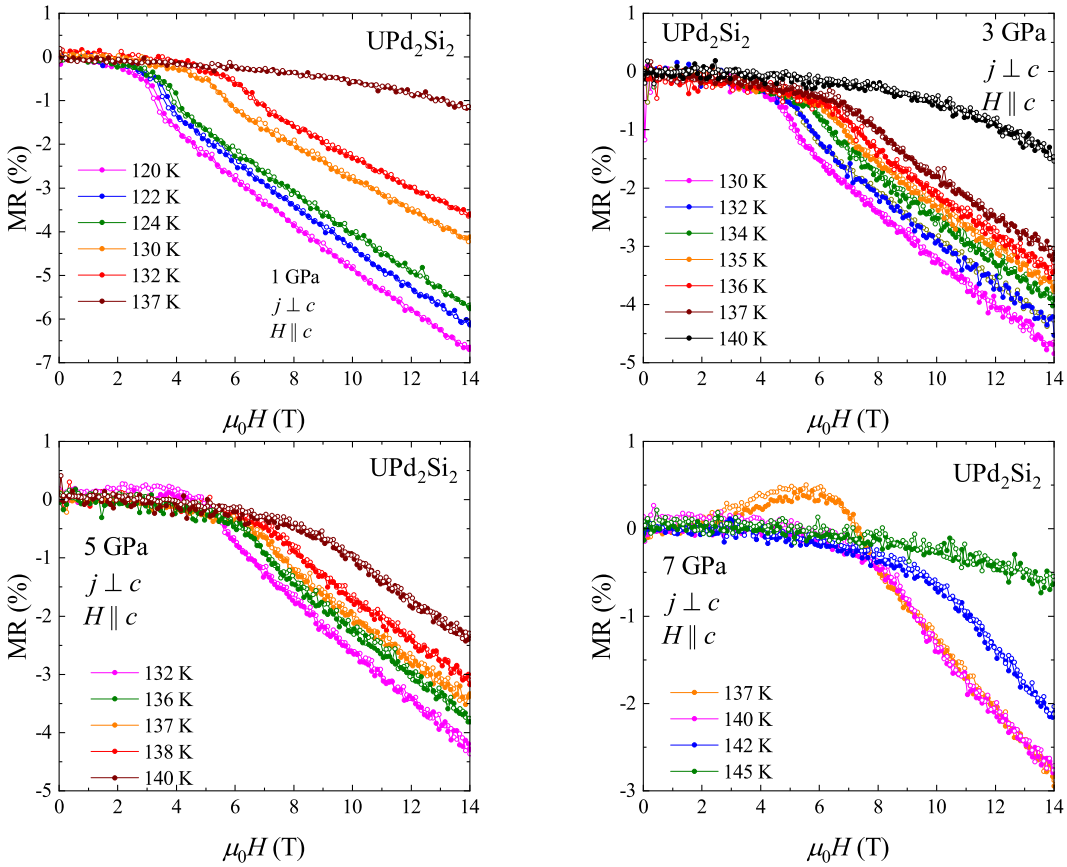


FIG. 6. Field dependencies of the magnetoresistivity of single-crystal $UPd_2Si_2$, measured with $j \perp c$ and $B \parallel c$ at different temperatures above $T_{\text{IC-AFM}}$, in high pressures. Solid and open symbols denote variations measured with increasing and decreasing magnetic field, respectively.

to 9 T [30]). Under pressure of 7 GPa, the MR($H$) variations have a somewhat different character. At low temperatures, the compound remains in the AFM state up to 14 T, and MR($H$) measured at 60 K does not show any distinct feature. A slight increase in MR is observed at 80 K, however, the critical field cannot be determined, as up to 14 T, only the onset of the transition is visible. At 100 K, the whole hysteresis loop associated with the metamagnetic transition can be observed. The critical field determined for the isotherm recorded just below $T_{\text{IC-AFM}}$ increases from 3 T (for 1 GPa and 115 K) to 8 T (for 7 GPa and 130 K). It should be noted that the magnetoresistivity measured at 3 GPa at 100 and 110 K shows a slight bifurcation between variations recorded with increasing and decreasing magnetic field, the origin of which is unclear.

The magnetoresistivity isotherms recorded above $T_{\text{IC-AFM}}$ under different pressures are displayed in Fig. 6. For each pressure, the critical field, determined as a drop in MR($H$), increases with increasing temperature up to the Néel temperature. Noticeably, as the pressure increases, the shape of the curves measured at higher temperatures changes. While that measured at 137 K under 1 GPa shows no features and is typical of paramagnets, the MR($H$) variation recorded at the same temperature under pressure of 3 GPa shows a clear metamagnetic transition, thus confirming that the system is in an ordered IC state. The same behavior occurs in the curves measured at 140 K under pressure of 3 and 5 GPa. Under 7 GPa, the magnetic order is seen even at $T = 142$ K. This finding agrees with the shift of the Néel temperature with increasing pressure, found in the present study, yet not observed in previous investigations [29]. Due to the change in the position of TP, similarly as for the variations taken below $T_{\text{IC-AFM}}$, the MR($H$) isotherms are shifted towards higher magnetic fields.

## IV. MAGNETIC PHASE DIAGRAMS AND CONCLUSIONS

Based on the afore-discussed magnetotransport data, collected on single-crystalline $UPd_2Si_2$ in wide ranges of temperature, magnetic field and pressure, the magnetic $H$-$T$ phase diagrams were constructed (see Fig. 7). For completeness, our results obtained at ambient pressure [30], as well as those reported in Ref. [22], are also shown in this figure. Contrary to previous reports [29], the application of pressure does not lead to merging the PM-IC and AFM-IC transition lines up to 7 GPa. Moreover, the PM-IC and FIM-IC phase boundaries between do not meet up to 14 T and up to the highest pressures studied. Possibly, higher pressures or higher magnetic fields are necessary to reach LP in the magnetic phase diagram of $UPd_2Si_2$.

Another important feature of the high-pressure $H$-$T$ diagrams constructed for the compound is that hydrostatic pressure stabilizes the AFM phase. First of all, in zero magnetic field, a rise was found in the temperature of the transition between the IC and AFM states, from 108 K at ambient

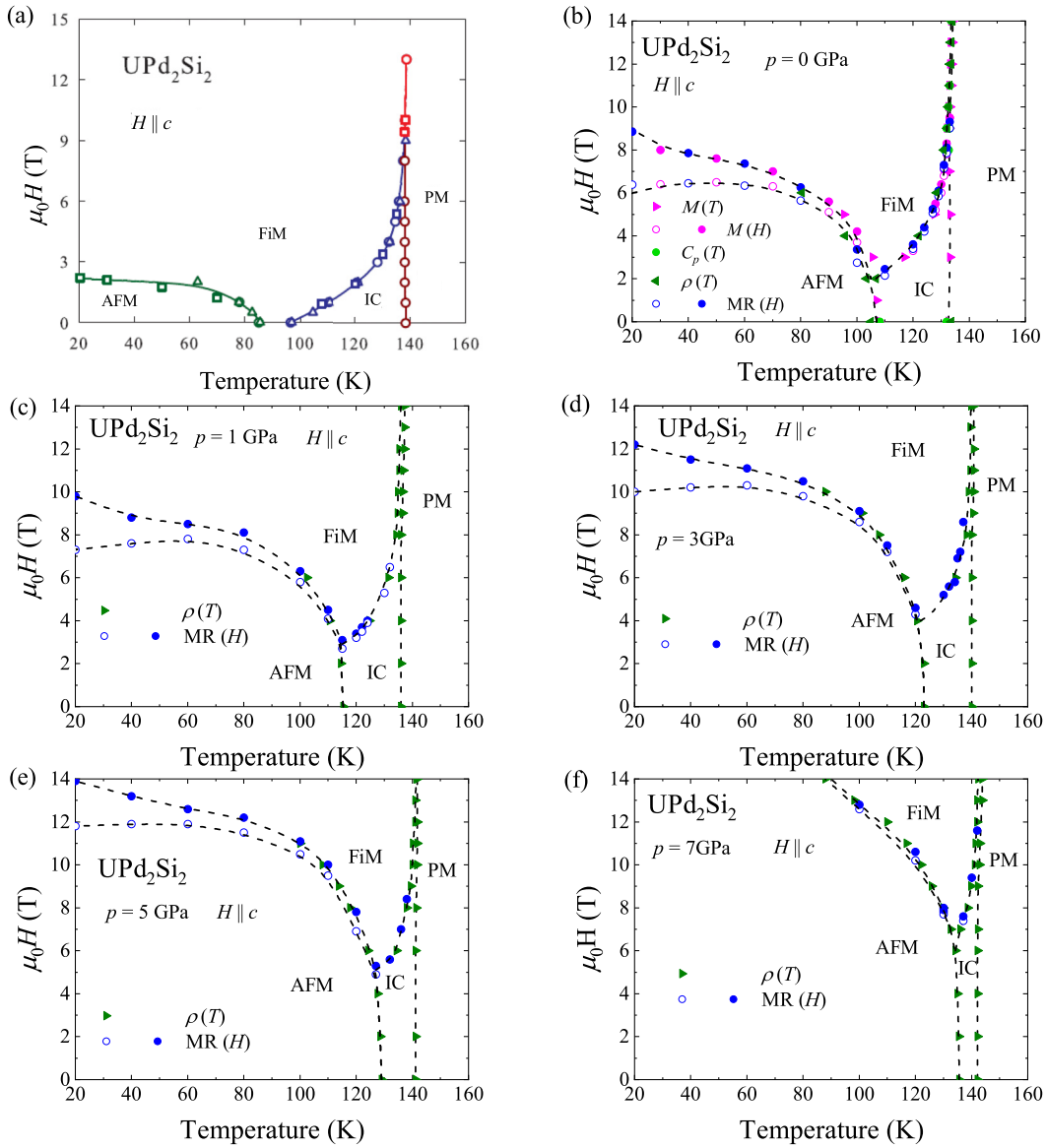


FIG. 7. (a) Magnetic phase diagram of $UPd_2Si_2$ at ambient pressure, reported in Ref. [22]. (b) Magnetic phase diagram of $UPd_2Si_2$ at ambient pressure, reported in our companion paper [30]. (c)–(f) Magnetic phase diagrams of $UPd_2Si_2$ for high pressures up to 7 GPa. For (b)–(f) solid and open symbols denote the data obtained with increasing and decreasing fields, respectively.

pressure to 136 K under a pressure of 7 GPa. Furthermore, at low temperatures, the application of pressure brings about an increase of the critical field of the transition between the AFM and FIM states (at 20 K, it is equal to about 10 T at ambient pressure and 14 T under 5 GPa). At 7 GPa, $UPd_2Si_2$ remains antiferromagnetic up to 14 T. The triple point, where the three ordered phases IC, AFM, and FIM meet, observed at about 106 K and below 2 T at ambient pressure, is systematically shifted with increasing pressure to higher fields and temperatures, and TP is observed at 135 K and above 6 T for the pressure 7 GPa.

Finally, it should be recalled here the magnetic phase diagram of $UPd_2Si_2$ reported by Plackowski *et al.* in Ref. [22] and reproduced in Fig. 7(a), in which all three ordered phases are observed in zero magnetic field, and hence no TP associated with the AFM- FiM and IC-FIM transitions occurs. Compared to the crystal studied in the present work and also that reported in Ref. [21], the AFM phase observed in Ref. [22] is less stable, and the critical field of the transition between the AFM and FIM phases is much smaller. Generally, comparing the individual $H$-$T$ diagrams shown in Fig. 7, it is possible to speculate that the behavior of the crystal studied by Plackowski *et al.* corresponds to that expected for the crystal from Fig. 7(b) subjected to "negative pressure." To verify this tempting hypothesis, high-pressure experiments on the crystal type studied in Ref. [22] should be conducted. It remains an open question what causes the differences between the $UPd_2Si_2$ crystals whose ambient pressure magnetic phase diagrams are shown in Figs. 7(a) and 7(b). It is worth recalling that a very accurate description of them was obtained using an axial next-nearest-neighbor Ising (ANNNI) model that took into account ferromagnetic in-plane interactions $J_0$,

antiferromagnetic near-neighbor $J_1$, next-near neighbor $J_2$ interactions, and a small ferromagnetic third-neighbor interaction $J_3$ [32]. Whether the FIM phase appears in zero field or upon applying magnetic field depends on small differences in the ratio of the exchange parameters $J_1$ and $J_2$. It seems reasonable to consider that this ratio is controlled by tiny structural features, such as minute nonstoichiometry or atomic disorder, which have been recognized to being fairly common in the $UT_2X_2$ ($T = d$-electron transition metal; $X =$ Si or Ge) compounds [33,34].

## ACKNOWLEDGMENT

The work was supported by Narodowe Centrum Nauki (National Science Center, Poland) within scientific project SONATA-14 2018/31/D/ST3/03295.

[1] R. M. Hornreich, M. Luban, and S. Shtrikman, Critical behavior at the onset of $\vec{k}$-space instability on the λ line, Phys. Rev. Lett. **35**, 1678 (1975).

[2] R. Hornreich, The Lifshitz point: Phase diagrams and critical behavior, J. Magn. Magn. Mater. **15**, 387 (1980).

[3] Y. Shapira, C. C. Becerra, N. F. Oliveira, and T. S. Chang, Phase diagram, susceptibility, and magnetostriction of MnP: Evidence for a Lifshitz point, Phys. Rev. B **24**, 2780 (1981).

[4] A. Szytuła, Magnetic properties of 1:2:2 rare-earth and actinide intermetallics, J. Alloys Compd. **181**, 123 (1992).

[5] T. T. M. Palstra, A. A. Menovsky, G. J. Nieuwenhuys, and J. J. Mydosh, Magnetic properties of the ternary compounds $CeT_2Si_2$ and $UT_2Si_2$, J. Magn. Magn. Mater. **54**, 435 (1986).

[6] Y. Dalichaouch, M. B. Maple, M. S. Torikachvili, and A. L. Giorgi, Ferromagnetic instability in the heavy-electron compound $URu_2Si_2$ doped with Re or Tc, Phys. Rev. B **39**, 2423 (1989).

[7] T. D. Matsuda, N. Metoki, Y. Haga, S. Ikeda, K. Kaneko, E. Yamamoto, and Y. Ōnuki, Crystal and magnetic structure in the itinerant 5f antiferromagnet $UCr_2Si_2$, J. Phys.: Condens. Matter **15**, S2023 (2003).

[8] T. D. Matsuda, N. Metoki, Y. Haga, S. Ikeda, T. Okubo, K. Sugiyama, N. Nakamura, K. Kindo, K. Kaneko, A. Nakamura, E. Yamamoto, and Y. Ōnuki, Single crystal growth and structural and magnetic properties of the uranium ternary intermetallic compound $UCr_2Si_2$, J. Phys. Soc. Jpn. **72**, 122 (2003).

[9] A. Szytuła, S. Siek, J. Leciejewicz, A. Zygmunt, and Z. Ban, Neutron diffraction study of $UT_2X_2$ (T = Mn, Fe, X = Si, Ge) intermetallic systems, J. Phys. Chem. Solids **49**, 1113 (1988).

[10] L. Chełmicki, J. Leciejewicz, and A. Zygmunt, Magnetic properties of $UT_2Si_2$ and $UT_2Ge_2$ (T = Co, Ni, Cu) intermetallic systems, J. Phys. Chem. Solids **46**, 529 (1985).

[11] P. Svoboda, P. Javorský, V. Sechovský, A. Menovsky, M. Hofmann, and N. Stüsser, Magnetic phase diagram and critical scattering of $UNi_2Si_2$, Phys. B: Condens. Matter **322**, 248 (2002).

[12] T. D. Matsuda, Y. Haga, S. Ikeda, A. Galatanu, E. Yamamoto, H. Shishido, M. Yamada, J.-I. Yamaura, M. Hedo, Y. Uwatoko, T. Matsumoto, T. Tada, S. Noguchi, T. Sugimoto, K. Kuwahara, K. Iwasa, M. Kohgi, R. Settai, and Y. Ōnuki, Electrical and magnetic properties of a single crystal $UCu_2Si_2$, J. Phys. Soc. Jpn. **74**, 1552 (2005).

[13] R. Troć, Z. Gajek, A. Pikul, H. Misiorek, E. Colineau, and F. Wastin, Phenomenological crystal-field model of the magnetic and thermal properties of the Kondo-like system $UCu_2Si_2$, Phys. Rev. B **88**, 024416 (2013).

[14] A. J. Dirkmaat, T. Endstra, E. A. Knetsch, G. J. Nieuwenhuys, J. A. Mydosh, A. A. Menovsky, F. R. de Boer, and Z. Tarnawski, Magnetic, thermal, and transport properties of $UIr_2Si_2$, Phys. Rev. B **41**, 2589 (1990).

[15] R. A. Steeman, E. Frikkee, S. A. M. Mentink, A. A. Menovsky, G. J. Nieuwenhuys, and J. A. Mydosh, Hybridisation effects in $UPt_2Si_2$, J. Phys.: Condens. Matter **2**, 4059 (1990).

[16] C. Tabata, N. Miura, K. Uhlířova, M. Vališka, H. Saito, H. Hidaka, T. Yanagisawa, V. Sechovský, and H. Amitsuka, Peculiar magnetism of $UAu_2Si_2$, Phys. Rev. B **94**, 214414 (2016).

[17] A. Vernière, S. Raymond, J. Boucherle, P. Lejay, B. Fåk, J. Flouquet, and J. Mignot, Magnetic structure and physical properties of the heavy fermion $UIr_2Si_2$, J. Magn. Magn. Mater. **153**, 55 (1996).

[18] A. Vernière, P. Lejay, J. Boucherle, J. Muller, S. Raymond, J. Flouquet, and A. Sulpice, Low temperature structural and physical behaviour of $UIr_2Si_2$ single crystal, Phys. B: Condens. Matter **206-207**, 509 (1995).

[19] M. Szlawska, M. Majewicz, D. A. Kowalska, and D. Kaczorowski, Metamagnetic transition in single-crystalline $UIr_2Si_2$, Sci. Rep. **13**, 14772 (2023).

[20] J. A. Mydosh, P. M. Oppeneer, and P. S. Riseborough, Hidden order and beyond: an experimental—theoretical overview of the multifaceted behavior of $URu_2Si_2$, J. Phys.: Condens. Matter **32**, 143002 (2020).

[21] T. Honma, H. Amitsuka, S. Yasunami, K. Tenya, T. Sakakibara, H. Mitamura, T. Goto, G. Kido, S. Kawarazaki, Y. Miyako, K. Sugiyama, and M. Date, Incommensurate-commensurate magnetic phase transitions of the Ising-5$f$ system $UPd_2Si_2$: the $H$-$T$ phase diagram and mean-field analyses, J. Phys. Soc. Jpn. **67**, 1017 (1998).

[22] T. Plackowski, D. Kaczorowski, and J. Sznajd, Magnetic phase diagram and possible Lifshitz critical point in $UPd_2Si_2$, Phys. Rev. B **83**, 174443 (2011).

[23] A. Amorese, M. Sundermann, B. Leedahl, A. Marino, D. Takegami, H. Gretarsson, A. Gloskovskii, C. Schlueter, M. W. Haverkort, Y. Huang, M. Szlawska, D. Kaczorowski, S. Ran, M. B. Maple, E. D. Bauer, A. Leithe-Jasper, P. Hansmann, P. Thalmeier, L. H. Tjeng, and A. Severing, From antiferromagnetic and hidden order to Pauli paramagnetism in $UM_2Si_2$ compounds with 5$f$ electron duality, Proc. Natl. Acad. Sci. USA **117**, 30220 (2020).

[24] H. Ptasiewicz-Bąk, J. Leciejewicz, and A. Zygmunt, Neutron diffraction study of magnetic ordering in $UPd_2Si_2$, $UPd_2Ge_2$, $URh_2Si_2$ and $URh_2Ge_2$, J. Phys. F: Met. Phys. **11**, 1225 (1981).

[25] B. Shemirani, H. Lin, M. F. Collins, C. V. Stager, J. D. Garrett, and W. J. L. Buyers, Magnetic structure of $UPd_2Si_2$, Phys. Rev. B **47**, 8672 (1993).

[26] M. F. Collins, B. Shemirani, C. V. Stager, J. D. Garrett, H. Lin, W. J. L. Buyers, and Z. Tun, Magnetic structure

of $UPd_2Si_2$ in a magnetic field, Phys. Rev. B **48**, 16500 (1993).

[27] G. Quirion, F. S. Razavi, M. L. Plumer, and J. D. Garrett, Pressure-temperature phase diagram of $UPd_2Si_2$ and $UNi_2Si_2$, Phys. Rev. B **57**, 5220 (1998).

[28] C. Sekine, K. Kihou, T. Inaba, T. Togashi, I. Shirotani, and T. Honma, Study of electrical resistivity on strongly correlated electron antiferromagnet at low temperature, high pressure and high magnetic field, Mem. Muroran Inst. Technol. **49**, 105 (1999).

[29] H. Hidaka, A. Tanaka, S. Takahashi, T. Yanagisawa, and H. Amitsuka, Pressure-induced bicritical point in $UPd_2Si_2$, J. Phys.: Conf. Ser. **273**, 012032 (2011).

[30] M. Szlawska, M. Majewicz, K. Wochowski, and D. Kaczorowski, preceding paper, Hunt for a Lifshitz point in single-crystalline $UPd_2Si_2$. I. High magnetic fields, Phys. Rev. B **110**, 014434 (2024).

[31] M. Ohashi and G. Oomi, Simple experimental procedure under quasi-hydrostatic pressure up to 15 GPa at low temperature, Jpn. J. Appl. Phys. **48**, 070221 (2009).

[32] M. L. Plumer, Mean-field phase diagrams of $AT_2X_2$ compounds, Phys. Rev. B **50**, 13003 (1994).

[33] S. Süllow, S. A. M. Mentink, T. E. Mason, R. Feyerherm, G. J. Nieuwenhuys, A. A. Menovsky, and J. A. Mydosh, Disorder to order transition in the magnetic and electronic properties of $URh_2Ge_2$, Phys. Rev. B **61**, 8878 (2000).

[34] S. Süllow, A. Otop, A. Loose, J. Klenke, O. Prokhnenko, R. Feyerherm, R. W. A. Hendrikx, J. A. Mydosh, and H. Amitsuka, Electronic localization and two-dimensional metallic state in $UPt_2Si_2$, J. Phys. Soc. Jpn. **77**, 024708 (2008).